COMPARISON OF FINE NEEDLE BIOPSY CYTOLOGICAL IMAGE SEGMENTATION METHODS

Maciej Hrebień, Piotr Steć and Józef Korbicz
Institute of Control and Computation Engineering, University of Zielona Góra
ul. Podgórna 50, 65-246 Zielona Góra, Poland

Keywords: Cytology, image processing, segmentation.

Abstract: This paper describes an early stage of cytological image recognition and presents a comparision of two hybrid segmentation methods. The analysis includes the Hough transform with conjunction to the watershed algorithm and with conjunction to the active contours techniques. One can also find here a short description of image pre-processing and an automatic nucleuses localization mechanisms used in our approach. Preliminary experimental results collected on a hand-prepared benchmark database are also presented with short discussion of common errors and possible future problems.

1 INTRODUCTION

Construction of a fully automatic cancer diagnosis system is a challenging task. In last decade we can observe a very dynamic growth in number of researches conducted in this area not only by university centers but also by commercial institutions (Kimmel et al., 2003). Because the breast cancer is becoming most common disease of the present female population, much attention of the present-day researchers is directed to this issue. The attention covers not only curing the external effects of the disease but also its fast detection in its early stadium.

The nucleus of the cell is the place where breast cancer malignancy can be observed. Therefore, it is crucial for any camera based automatic diagnosis system to separate the cells and their nuclei from the rest of the image content. Until now many segmentation methods were proposed (Gonzalez and Woods, 2002; Pratt, 2001; Russ, 1999) but unfortunately each of them introduces different kinds of additional problems and usually works in practice under given assumptions and/or needs end-user's interaction/cooperation. Since many cytological projects assume rather full automation and real-time operation with high degree of efficacy, a method free of drawbacks of already known approaches has to be constructed.

In this paper two hybrid methods of cytological image segmentation are presented, that is the Hough transform with conjunction to the watershed algorithm and with conjunction to the active contours techniques. One can also find here a short description of image pre-processing and fully automatic nuclei localization mechanisms used in our approach.

2 PROBLEM FORMULATION

Mathematical formulation of the segmentation process is very difficult because it is a poorly conditioned problem. Thus we give here only some informal definition of the problem we have to face.

What we have on input is a cytological material obtained using the Fine Needle Biopsy technique and imagined with a *Sony CCD Iris* camera mounted atop of an *Axiophot* microscope. The material comes from female patients of Zielona Góra's *Onkomed* medical center (Marciniak et al., 2005). The 704×576 pixel image itself is coded using the RGB colourspace and is not subject of any kind of lossy compression.

What we expect on output is a binary segmentation mask with one pixel separation rule which will allow us to more robust morphometric parameters estimation in our future work. Additionally, the algorithm should be insensitive to colours of contrasting

Hrebień M., Steć P. and Korbicz J. (2007).
COMPARISON OF FINE NEEDLE BIOPSY CYTOLOGICAL IMAGE SEGMENTATION METHODS.
In *Proceedings of the Fourth International Conference on Informatics in Control, Automation and Robotics*, pages 305-310
DOI: 10.5220/0001645603050310

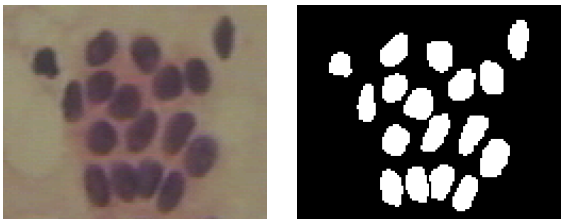

(a) (b)

Figure 1: Exemplary fragment of: (a) cytological image, (b) appropriate segmentation mask.

pigments used for preparation of the cytological material (see an example in Fig. 1).

3 IMAGE PRE-SEGMENTATION

3.1 Pre-processing

The colour components of an image do not carry as important information as the luminosity does, so they can be removed to reduce processing complexity in stages that require only e.g. gradient estimations. An RGB colour image can be converted to greyscale by removing blue and red chrominance components from the image defined in YCbCr colour space (Pratt, 2001).

Since the majority of images we deal with have low contrast, an enhancement technique is needed to improve their quality. In our approach we use simple histogram processing with linear transform of image levels of intensities, that is the cumulated sum approach (Russ, 1999). The contrast correction operation is conducted for each colour channel separately resulting in an image being better-defined for later stages of the presented hybrid segmentation methods (see Fig. 2).

3.2 The Background of the Algorithm

If we look closely at the nuclei we have to segment, they all have elliptical shape. Most of them remind ellipse but unfortunately detection of ellipse which is described by two parameters a and b ($x = a\cos\alpha$, $y = b\sin\alpha$) and which can be additionally rotated is computationally expensive. The shape of ellipse can be approximated by a given number of circles. Detection of circles is much more simpler in the sense of required computations because we have only one parameter, that is the radius R. This observations and simplifications constitute grounding for fast nucleus pre-segmentation algorithm – in our approach we try

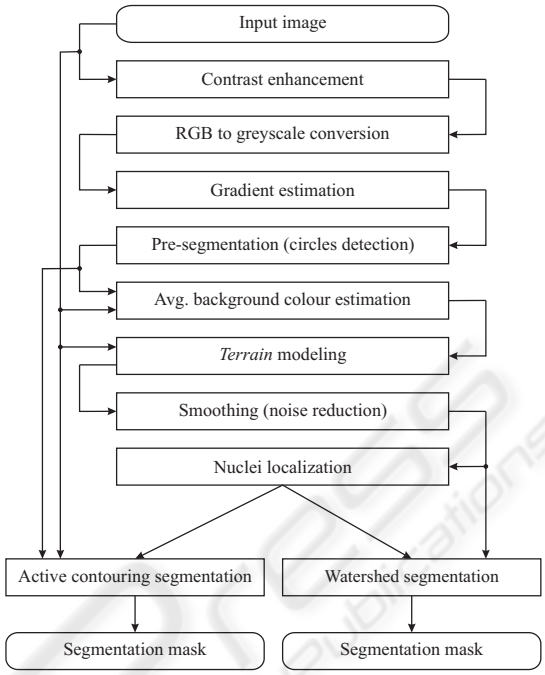

Figure 2: Flow graph of the presented solutions.

to find such circles with different radii in a given feature space.

3.3 Circles Detection

The Hough transform (Toft, 1996; Żorski, 2000) can be easily adopted for the purpose of circle detection. The transform in the discrete space can be defined as:

$$HT_{discr}(R,\hat{i},\hat{j}) = \sum_{i=\hat{i}-R}^{\hat{i}+R}\sum_{j=\hat{j}-R}^{\hat{j}+R} g(i,j)\delta\Big((i-\hat{i})^2+(j-\hat{j})^2-R^2\Big), \quad (1)$$

where g is a two dimensional feature image and δ is the Kronecker's delta (equal to unity at zero) which defines sum only over the circle. The HT_{discr} plays the role of accumulator which accumulates levels of feature image g similarity to circle placed at the $(\hat{i},\hat{j})$ position and defined by the radius R.

The feature space g can be created by many different ways. In our approach we use gradient image as the feature indicating nucleus' occurrence or absence in a given fragment of cytological image. The gradient image is a saturated sum of gradients estimated in eight directions on greyscale image prepared in the pre-processing stage. The base gradients can be calculated using e.g. Prewitt's, Sobel's mask methods or

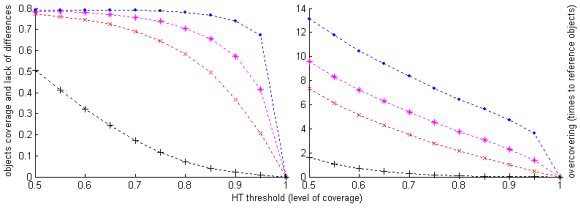

Figure 3: Influence of θ threshold value on objects's cover and lack of differences (left) and overcovering (right) for Prewitt (×), Sobel (∗), heavy (•) and light (+) base gradient masks (experiments performed on a randomly selected 346 element Zielona Góra's *Onkomed* (Marciniak et al., 2005) cytological benchmark database for radii in the 4-21 pixel range).

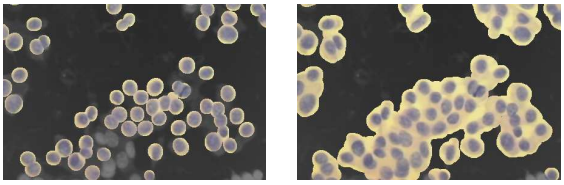

(a) (b)

Figure 4: Exemplary results of the pre-segmentation stage for two different θ threshold strategies: (a) high and (b) low.

their heavy or light versions (Gonzalez and Woods, 2002; Tadeusiewicz, 1992).

3.4 Final Actions

Thresholding the values in the accumulator by a given θ value can lead us to a very good pre-segmentation mechanism with the lower threshold strategy (see for instance Fig. 4). Since the threshold value strongly depends on the database and used feature image g (Fig. 3), the method can only be used as a pre-segmentation stage. Smaller value of the threshold causes fast removal of non-important information from the background what can constitute a base for more sophisticated and going into details algorithms.

4 IMAGE SEGMENTATION

4.1 *Terrain* Modeling

The results obtained from the pre-segmentation stage can lead us to the estimation of average background colour. This information can be used to model the nuclei as a colour distance between background and objects what fulfils requirements of lack of any colour

(a) (b) (c)

Figure 5: Exemplary fragment of: (a) cytological image, (b) Euclidian distance to the mean background colour, (c) smoothed out version of (b).

dependency in imaged material (the colour of contrasting pigments may change in the future). In our research we tried few distance metrics: Manhattan's, Chebyshev's, absolute Hue value from HSV colourspace but Euclidian one gives the best visual results (Fig. 5ab).

Since the modeling distance can vary in local neighborhood (see Fig. 5b) mostly because of camera sensor simplifications, a smoothing technique is needed to reconstruct the nuclei shape. The smoothing operation in our approach relies on the fact that this sort of 2D signal can be modeled as a sum of sinusoids (Madisetti and Williams, 1997) with defined amplitudes, phase shifts and frequencies. Cutting all low amplitude frequencies off (leaving only a few significant ones with the highest amplitude) will result in a signal deprived our problematic local noise effect (Fig. 5c).

4.2 Nuclei Localization

Localization of objects on a modeled map of nuclei can be performed locally using various methods. In our approach we have chosen evolutionary (1+1) search strategy (Arabas, 2004) mostly because it is simple, quite fast despite appearances, can be easily parallelized due to its nature and it settles very good in local extrema what is very important in our case.

The used watershed segmentation algorithm forced us to create two population of individuals. The first population is localizing the background. Specimens are moved with a constant movement step equal to unity and the movement is preferred to the places with a smaller density of population to maximize background coverage. The second population is localizing the nuclei. Specimens are moved with a exponentially decreasing movement step to very fast group the population near local extrema in first few epochs and to finally work on details in the ending ones. The movement of individuals is preferred to the places with a higher population density to create the effect of nuclei localization.

The change for the better position of an individ-

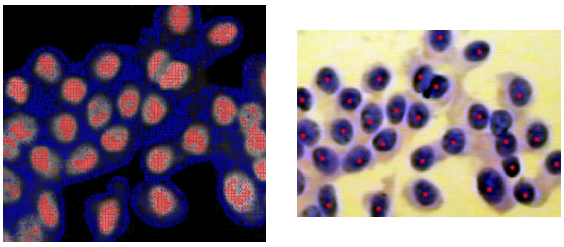

(a) (b)

Figure 6: Exemplary localization: (a) screenshot after 8 epochs, (b) final result (localization points are marked with red asterisks).

ual searching for nuclei is calculated as a product of randomly generated distance with normal distribution $N(0,1)$ and an decreasing in time radius $r^t = R_{max}\left(\frac{1}{R_{max}}\right)^{\frac{t}{t_{max}}}$, where R_{max} is the maximal radius detected by the Hough transform. Specimens covering background are generated in a similar way except $R = 1$ during mutation.

The fitness function calculates the average *height* of the terrain in a given position including nearest neighborhood defined by the smallest radius detected by the Hough transform in the pre-segmentation stage. Such definition of the fitness function avoids a possible split of population, localized near a nucleus with multimodal character of its shape, giving only one marker for a nucleus (Fig. 6b).

Finally, the nucleus is localized in the place where the density of the population searching for hilltops in the modeled terrain is locally maximal.

The used active contours techniques have lower requirements concerning nucleus localization. In this approach it is allowed to have more than one marker pointing the same nucleus. Thus the localization algorithm in this case can be much simplified. We need only one population, that is the one searching for nuclei and the fitness function is simply the terrain *height* at an individuals position. Additionally, it is allowed to have not optimal or even false localization points what reduces number of needed iterations of the algorithm.

4.3 Building Watersheds

The watershed segmentation algorithm is inspired by natural observations, that is a rainy day in mountains (Gonzalez and Woods, 2002; Pratt, 2001; Russ, 1999). A given image can be defined as a terrain on which nuclei correspond to valleys (upside down terrain modeled in previous steps). The terrain is flooded by rainwater and arising puddles are starting to turn into basins. When the water from one basin begins to pour away to another, a separating watershed is created.

The flooding operation have to be stopped when the water level reaches a given θ threshold. The threshold should preferably be placed somewhere in the middle between the background and a nucleus localization point. In our approach nuclei are flooded to the half of the altitude between nucleus localization point and the average height of the background in the local neighborhood. Since the images we have to deal with are spot illuminated during imaging operation (resulting in a modeled terrain being higher in the center of the image and much lower in the corners) this mechanism protects the basins against being overflooded and in consequence nuclei being undersegmented. To satisfy the one pixel separation rule the algorithm needs to have multi-label extension and the watersheds are built only when there is a neighbor nearby with other label.

4.4 Active Contours

An active contour segmentation is performed using multilabel fast marching algorithm presented in (Steć, 2005; Hrebień and Steć, 2006) which is extension to the original fast marching method (FMM) developed by Sethian (Sethian, 1998). The problem with the original FMM is that the contour can be moved only in one direction. This means that any error in segmentation cannot be corrected and algorithm requires additional stop condition. To deal with this problem, multilabel extension to the classical FMM was proposed.

Initialization of the multilabel fast marching is done in similar way as it was done for the watershed algorithm. The difference is that the watershed initialization image requires an additional processing to leave exactly one seed per nucleus while the FMM allows more seeds in one nucleus. Similar method of initialization will allow direct comparison of the segmentation results.

Initial contour propagation is similar to original FMM method. Expansion of the contour is governed by a propagation speed defined globally for all the contours. Speed is based on the difference between mean colour in the initialization area and colour of the pixel under the contour:

$$F = \frac{1}{|g(x,y) - \bar{g}(i)|^3 + 1}, \qquad (2)$$

where $g(x,y)$ is the colour under the contour and $\bar{g}(i)$ is the mean colour under the i-th segment. Such a speed definition slows down the contour near the de-

tected object boundary what increases probability of contours meeting near nucleus boundary.

When two segments meet, mean colour of the segments is compared. Comparison is taken at the point where contours start to overlap. When difference between mean colours from these two segments is below certain threshold segments are merged into one. To ensure maximum efficiency, labels from the smaller segment are changed to the value of those from the larger segment. Additionally, new mean colour for the segment is calculated from mean colours of connected segments.

If two segments that meet are not classified to be merged, the propagating segment can push back another segment under certain circumstances. At the meeting point differences between current pixel colour and mean colour of each segment is compared. Segment with lower difference value wins and replaces current label with its own. Replacement is performed as long as condition is meet. Contour that was pushed back cannot be propagated farther at places where its labels was replaced by another contour. Contour points that cannot be moved are no longer considered during calculations. Since contour can be pushed back only once, there is no oscillation at the object boundary known from the classical active contour methods. Additionally reduction of the contour length increases performance of the algorithm.

The presented algorithm stops propagation when all image points are assigned to segments and there is no segment that could push back another segment. The algorithm cannot run infinitely because oscillations between segments are impossible. No segment can visit twice the same area. Namely, when a segment was pushed back by another segment, it cannot get the lost pixels back.

4.5 Exemplary Results

Exemplary results of the presented watershed segmentation method and common errors observed on our hand-prepared benchmark database can be divided into four classes:

- *class 1*: good quality images with only small irregularities and rarely generated subbasins (basin in another basin) (Fig. 7ab),
- *class 2*: errors caused by fake circles created by spots of fat (Fig. 7cd),
- *class 3*: mixed nucleus types: red and purple in this case and those reds which are more purple than yellow (background) are also segmented what is erroneous (Fig. 7ef),

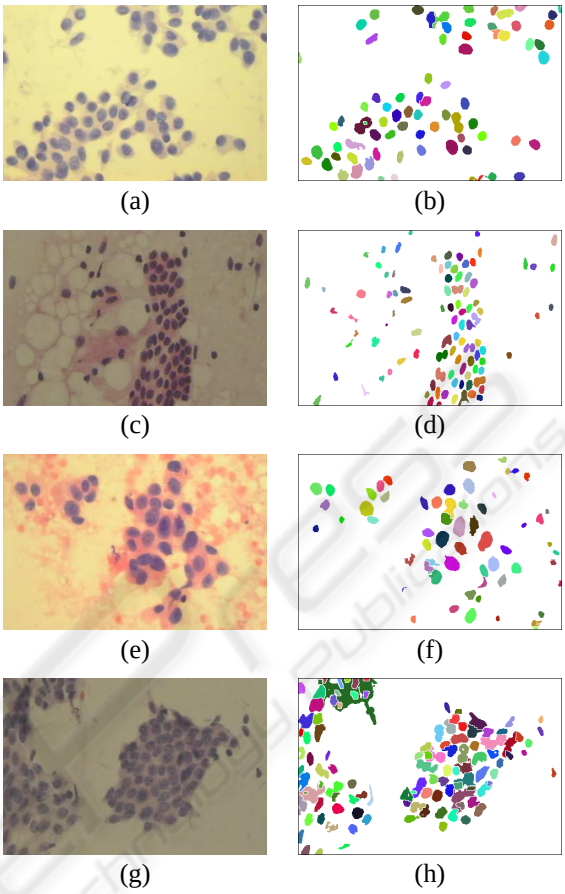

Figure 7: Exemplary results of the watershed segmentation.

- *class 4*: poor quality image with a bunch of nuclei glued together what causes basin's overflooding and in consequence undersegmentation (Fig. 7gh).

Conducted experiments show that the watershed algorithm gives 68.74% on the average agreement with the hand-prepared templates using simple XOR metric. As one can easily notice most errors are located at boundaries of nuclei (see for instance Fig. 8) where the average distance between edges of segmented and reference objects is about 3.28 pixles on the average. This causes the XOR metric to be underestimated as a consequence of not very heigh level of water flooding the modeled terrains. For the active contours algorithm the situation is very similar, that is the XOR metric gives 22.32% score and the average distance is equal to 4.1 pixels. Despite the underestimation fact the shape of nuclei seems to be preserved what is important for our future work, that is estimation of morphometric parameters of segmented nuclei.

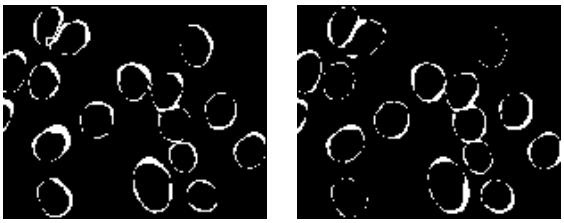

(a) (b)

Figure 8: Common XOR metric errors for: (a) the watershed and (b) the active contours method.

5 CONCLUSIONS

Conducted preliminary experiments show that the Hough transform adopted for circle detection in the pre-segmentation stage, the (1+1) search strategy used for automatic nuclei localization, the watershed algorithm and the active contours techniques used for the final segmentation stage can be effectively used for the segmentation of cytological images.

The problem regarding fake circles created by spots of fat and unwanted effects it gives in the final output should also be considered and eliminated in future work. Images with mixed nucleus type still constitute a challenge because it seems to be impossible to detect only one type without end-user's interaction and when there should not be any dependencies and assumptions concerning colour of contrasting pigments used to prepare cytological material. The proposal hybrid methods should also be extended to perform better on poor quality images or a fast classifier should be constructed to reject too poor (or even fake) inputs.

Summarizing, the presented solutions are promising and give a good base for our further research in the area of cytological image segmentation. Additionally, all preparation steps including pre-segmentation and the automatic nucleus localization stage can be reused with other segmentation algorithms which need such a information.

Performance of both algorithms is comparable. There was no result that clearly shows superiority of one algorithm above the other. The outcome was dependent on the used metric. Visually, segmentation results from both algorithms look very similar (see Fig. 8). Both algorithms have problems with the tight clusters of nuclei. They are usually detected as a single object.

Time reaction of both algorithms is similar too and it takes several seconds on today's PCs per image to give the final segmentation mask. All preparation steps are much more time consuming (2-3 minutes) but authors believe that it can be significantly reduced mostly because of the fact that this steps were simulated in MATLAB environment. Taking the advantage of today's multi-core machines, thread-oriented operating systems, the nature of used algorithms which are easy to parallelize and rewriting them using native code generating programming language can speed up the whole process significantly. A dedicated hardware could also be considered.

REFERENCES

Arabas, J. (2004). *Lectures on Evolutionary Algorithms*. WNT. (in Polish).

Gonzalez, R. and Woods, R. (2002). *Digital Image Processing*. Prentice Hall.

Hrebień, M. and Steć, P. (2006). The Hough transform and active contours in segmentation of cytological images. In *Proc. of the 9th Int. Conf. on Medical Informatics and Technology – MIT 2006*, pages 62–68, Wisła-Malinka, Poland.

Kimmel, M., Lachowicz, M., and Świerniak, A. (2003). Cancer growth and progression, mathematical problems and computer simulations. *Int. Journal of Appl. Math. and Comput. Science*, Vol. 13, No. 3, Special Issue.

Madisetti, V. and Williams, D. (1997). *The Digital Signal Processing Handbook*. CRC Press.

Marciniak, A., Obuchowicz, A., Mończak, R., and Kołodziński, M. (2005). Cytomorphometry of fine needle biopsy material from the breast cancer. In *Proc. of the 4th Int. Conf. on Comp. Recogn. Systems CORES'05*, Adv. in Soft Computing. Springer.

Pratt, W. (2001). *Digital Image Processing*. John Wiley & Sons.

Russ, J. (1999). *The Image Processing Handbook*. CRC Press.

Sethian, J. (1998). Fast Marching Methods and Level Set Methods for propagating interfaces. In *29th Computational Fluid Dynamics*, volume 1 of *VKI Lectures series*. von Karman Institute.

Steć, P. (2005). *Segmentation of Colour Video Sequences Using Fast Marching Method*, volume 6 of *Lecture Notes in Control and Computer Science*. University of Zielona Góra Press, Zielona Góra, Poland.

Tadeusiewicz, R. (1992). *Vision Systems of Industrial Robots*. WNT. (in Polish).

Toft, P. (1996). *The Radon Transform*. Technical University of Denmark. Ph.D. Thesis.

Żorski, W. (2000). *Image Segmentation Methods Based on the Hough Transform*. Studio GiZ Warszawa. (in Polish).